Compton profiles by inelastic ion-electron scattering

H. Böckl and F. Bell
Physics Section, University of Munich, D-8046 Garching, Germany
(Received 7 March 1983)

It is shown that Compton profiles (CP) can be measured by inelastic ion-electron scattering. Within the impulse approximation the binary-encounter peak (BEP) reflects the CP of the target atom whereas the electron-loss peak (ELP) is given by projectile CP's. Evaluation of experimental data reveals that inelastic ion-electron scattering might be a promising method to supply inelastic electron or photon scattering for the determination of target CP's. The measurement of projectile CP's is unique to ion scattering since one gains knowledge about wave-function effects because of the high excitation degree of fast heavy-ion projectiles.

I. INTRODUCTION

Very recently it has been demonstrated that the so-called binary-encounter peak (BEP) in ion-electron scattering can be used to extract Compton profiles (CP), i.e., projected momentum distributions of target electrons.[1,2] Whereas measurements of this kind are a well-established technique in inelastic electron-electron scattering,[3,4] the corresponding possibilities in ion-electron scattering have apparently not been recognized though they offer some advantage compared to electron-electron scattering. Especially in Ref. 1 it has been emphasized that Compton profiles from ion-electron scattering are by far less sensitive to multiple scattering than those from electron-electron scattering. It is the purpose of this paper to elucidate furthermore this technique by evaluating both our own experiments and those of other authors. Especially in the latter case it is shown that CP's with good accuracy are obtained though the experiments have been done without the aim to extract CP's.

In the following two paragraphs both the BEP and the electron-loss peak (ELP) are analyzed in terms of CP's. In the former case electrons from gas targets are ejected by the interaction with bare energetic ions, in the latter electrons are ejected from highly ionized projectile ions by the interaction with gas targets.

II. BINARY-ENCOUNTER PEAK

It has been demonstrated in Ref. 1 that in case of inelastic ion-electron scattering the double differential cross section (DDCS) for electron emission can be written (in a.u.)

$$\left[\frac{d^2\sigma}{dE\,d\Omega}\right]_{\mathrm{BEP}}=\frac{4Z_p^2}{v}k^{-3}\int d^3p\,|\psi_i(\vec{p})|^2\delta(\epsilon-(\vec{k}-\vec{p})\cdot\vec{v})$$

$$=\frac{1}{2v}\left[\frac{d\sigma}{d\Omega}\right]_R J_T(p_z)$$

with

$$J_T(p_z)=\int d^2p_\perp\,|\psi_i(p_\perp,p_z)|^2\,. \tag{1}$$

Here $\vec{k}$ is the final electron momentum ($E=\frac{1}{2}k^2$), Z_p the projectile charge, $\vec{p}$ the initial electron momentum, and ϵ the inelastic energy transfer. $J_T(p_z)$ is the so-called Compton profile of the target for a fixed z component of the intrinsic momentum $\vec{p}$. $(d\sigma/d\Omega)_R$ is the Rutherford cross section for an electron which receives a momentum transfer $\vec{k}$ by a projectile of velocity $\vec{v}$. Deriving Eq. (1) it has been assumed that $|\vec{k}|\gg|\vec{p}|$ and that the final electron state is approximated by a plane wave. The δ function of Eq. (1) keeps the z component of the intrinsic momentum $\vec{p}$ constant:

$$p_z v=kv\cos\theta-\tfrac{1}{2}k^2-|\epsilon_i|\,, \tag{2}$$

where θ is the electron emission angle and $|\epsilon_i|$ the electron binding energy. Equation (2) has several consequences on the behavior of the BEP. Its maximum is given by $p_z=0$, i.e., $E_{\max}=2v^2\cos^2\theta-2|\epsilon_i|$. Since usually the BEP is composed by several initial electron state contributions, each individual Compton profile is shifted by $2|\epsilon_i|$ to lower energies. This means in general asymmetric BEP's. The width of the BEP results from a kind of Doppler broadening, i.e., is given by $p_z v$ and thus is independent of the electron emission angle θ, in contrast to the BEP of electron-electron scattering.[4] Interestingly, Eq. (2) is a quadratic function of k which in turn leads to an extremum of the electron energy E as a function of p_z. Correspondingly the BEP has a minimum on the lower energy side whose position and depth is determined by the Rutherford cross section. Figure 1 shows the BEP for different projectile velocities v (in a.u.) according to Eq. (1). It is evident from Fig. 1 that the minimum is filled up with decreasing projectile velocity v until the peak is not visible any more. Figure 2 shows a collection of experimental results from Rudd *et al.*[5] and Toburen and Wilson[6] for protons on H_2. Figure 2 was taken from a review article of Rudd and Macek[7] and the data clearly corroborate the prediction of Fig. 1.

In the following we present CP's for He and Ar which we have gained from the experimental work of Rudd *et al.*[8] Figures 3 and 4 show CP's of He obtained by 1- and 1.5-MeV protons, respectively. Figures 5 and 6 represent Argon profiles by 1.5- and 3-MeV protons. For

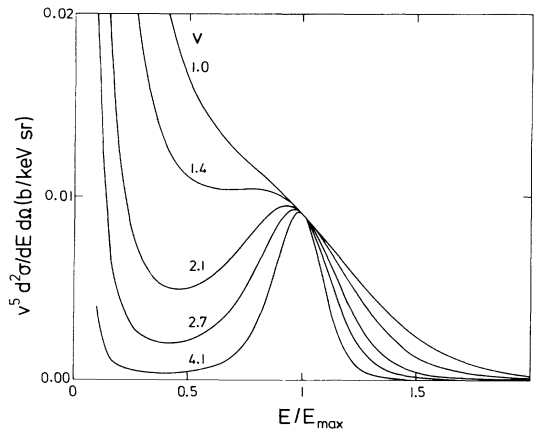

FIG. 1. BEP for different projectile velocities v (a.u.). Both double differential cross section $d^2\sigma/dE\,d\Omega$ and energy E are scaled in a suitable manner.

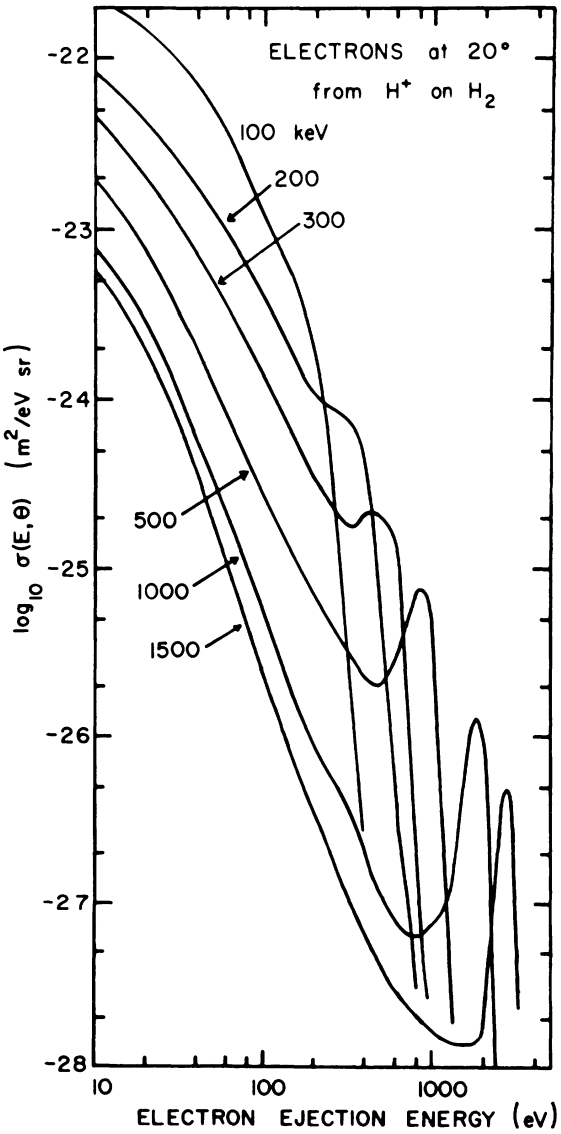

FIG. 2. Absolute electron emission cross sections for protons on H_2 from Ref. 7 which demonstrate the diminution of the BEP with decreasing projectile velocity.

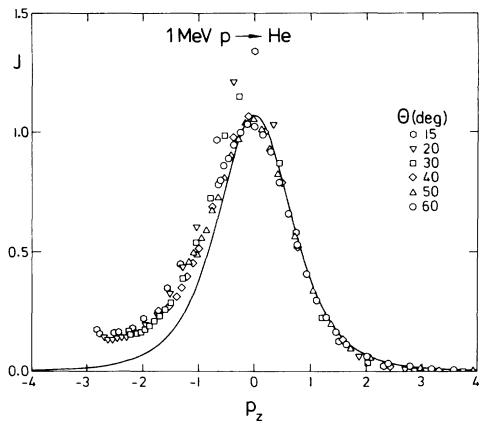

FIG. 3. Compton profile of He from 1-MeV protons and different electron emission angles θ, Ref. 8. Solid curve is a theoretical Compton profile from Ref. 9 which is based on Hartree-Fock calculations.

comparison the solid lines in Figs. 3 and 4 are CP's from Hartree-Fock calculations.[9] Figures 5 and 6 demonstrate the effect of asymmetry due to different shell contributions; whereas the broken curves are CP's without the incorporation of the binding energies $|\epsilon_i|$, the solid lines are CP's which include this binding effect. Figure 7 shows more clearly the individual shell contributions and their shift $|\epsilon_i|/v$. It is evident from Figs. 5 and 6 that the data favor the shifted profiles. It should be strongly emphasized that the comparison of experimental data and theoretical CP's in Figs. 3–6 is on an absolute scale: DDCS's of Ref. 8 and their energy scale have been converted to $J_T(p_z)$ and p_z without any adjustable parameter. This means that especially for the He data the absolute cross section must be correct within 5% which is an admirable accuracy.

Figure 4 suggests that the overall agreement between experimental data and theoretical CP's would be better if the theoretical profile is shifted slightly to lower p_z values. The reason for this difference could either be an experimental error of the energy calibration or a theoretical discrepancy which relies on the impulse approximation of Eq. (1). It is well known that both conventional photon

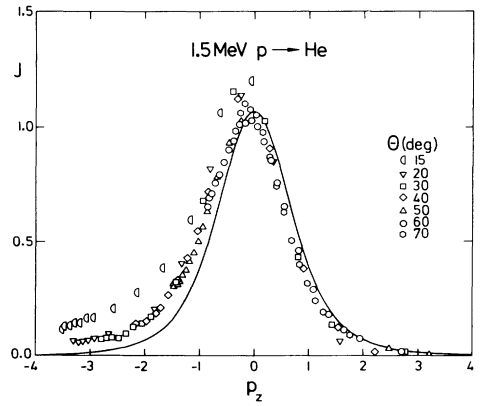

FIG. 4. Same as Fig. 3 but for 1.5-MeV protons.

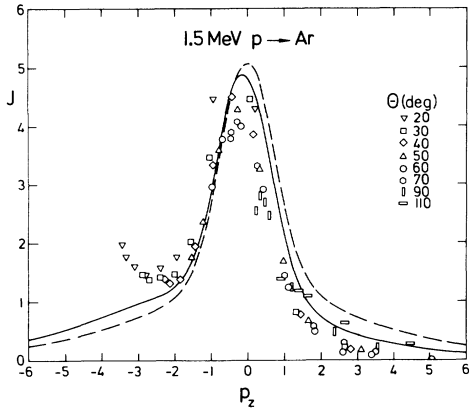

FIG. 5. Compton profile of Ar from 1.5-MeV protons and different electron emission angles θ, Ref. 8. The curves are theoretical Compton profiles from Ref. 9 which are based on Hartree-Fock calculations. Solid line: binding-energy shift included. Dashed line: without binding-energy shift.

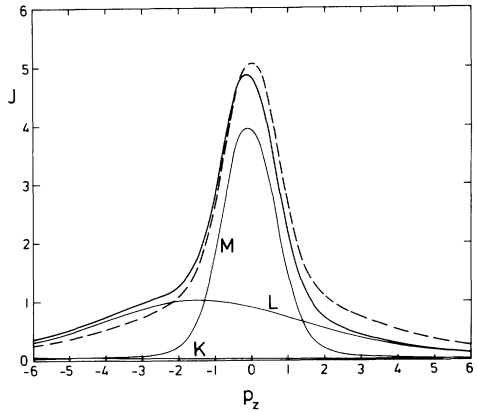

FIG. 7. Shell contributions to the total Compton profile of Ar. The individual contributions are shifted by $|\epsilon_i|/v$ and summed: solid line. Compton profile without binding-energy shift: dashed curve.

Compton scattering[10] and inelastic electron-electron scattering[11] lead to a so-called Compton defect, i.e., a deviation of the CP maximum from the value expected by the impulse approximation. Figure 8 shows that this effect occurs in ion-electron scattering, too. Here, we compare a hydrogeniclike CP of He (solid curve) and the CP due to Eq. (1) for which the DDCS had been calculated by the exact first Born approximation[12] with the same hydrogeniclike momentum distribution (broken curve). The Born approximation was calculated for 1.5-MeV protons at an emission angle $\theta=30°$. The corresponding momentum shift $|\epsilon_i|/v=0.258$ has been taken into account. The unusual behavior of the broken curve at negative p_z-values is a relic of the double-valued connection between p_z and k of Eq. (2) and signifies a break down of the impulse approximation. More important the comparison reveals a slight shift of the impulse approximation in analogy to the above-cited Compton defect. Though this shift has the same direction and is of the order of that in Fig. 4 it is doubtful if this is the correct interpretation since Fig. 5 does not show a comparable effect. Nevertheless, we found it worthwhile to mention this difference between the impulse approximation and the first Born approximation.

We should stress that in general the agreement between theoretical CP's and experimental data is quite good at the right side of the spectra whereas the lower energy side reveals a major discrepancy. It seems that this difference increases with decreasing emission angle θ. Figure 9 shows an example of our own work, where the CP of solid-state carbon has been obtained from 22-MeV protons. For experimental details see Ref. 1. In contrast to Ref. 1 the theoretical curve has been corrected for a slight change of the Rutherford cross section across the profile. It is seen that some unexplained intensity exists at the lower energy side also. The approximate representation of the final electron state by a plane wave might be improved by an additional Coulomb factor $2\pi\gamma[1-\exp(-2\pi\gamma)]^{-1}$ in Eq. (1) with $\gamma=Z_{\text{eff}}/k$. Here Z_{eff} is an effective charge of the target nucleus which determines the electron scattering in the final state. The rather good agreement between the theoretical CP and the experimental data points of Figs. 5 and 6 yields an upper limit $Z_{\text{eff}}=1$ for Ar. This small effective charge prohibits any strong

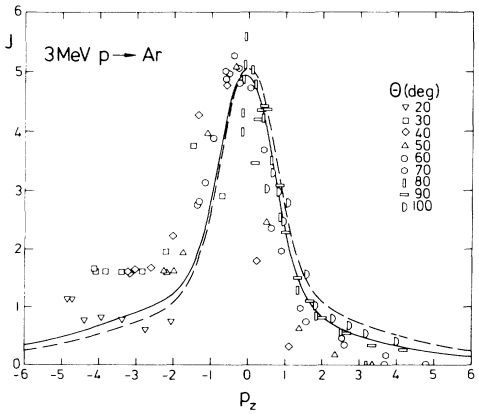

FIG. 6. Same as Fig. 5 but for 3-MeV protons.

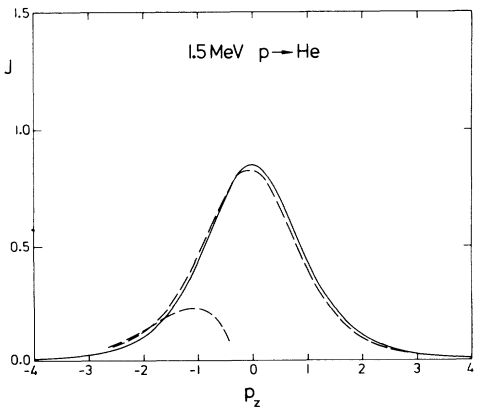

FIG. 8. Compton profile of He: solid line. Compton profile of He, deduced from Eq. (1) for a double differential cross section obtained from Ref. 1. Born approximation: dashed line.

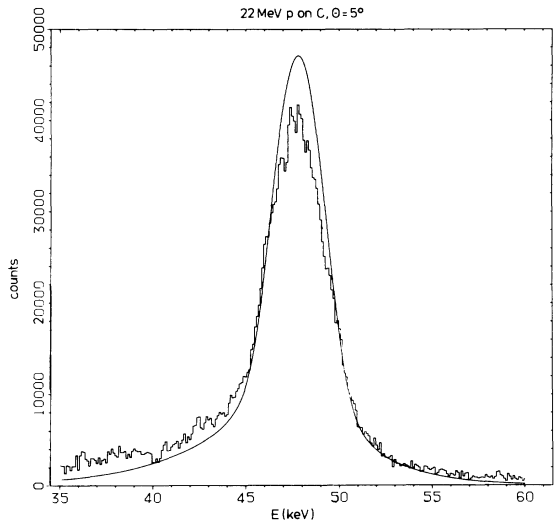

FIG. 9. BEP from 22-MeV protons on solid-state carbon at an emission angle $\theta=5°$. For comparison the double differential cross section due to Eq. (1) for a solid-state Compton profile (solid line). For details see Ref. 1.

change of the Coulomb factor across the CP which could explain the low-energy enhancement. In addition, the introduction of a similar Coulomb factor for electron scattering in the projectile field[13] could explain the angular behavior of the unknown intensity but fails quantitatively: The proton charge is too small to give any remarkable effect at the position of the BEP. Though there remain some unexplained features at the left side of the CP's, we believe that with increasing accuracy target CP's can be measured comparible to those from electron-electron scattering.

III. ELECTRON-LOSS PEAK

A further unique feature of ion-electron scattering is the possibility to obtain CP's from projectile ions in various stages of excitation. To do that one has to measure the ELP which occurs at $k=v$ and corresponds to the BEP in the projectile rest frame. It is easy to show that within the impulse approximation of Eq. (1) the corresponding DDCS for the ELP is given by

$$\left[\frac{d^2\sigma}{dE\,d\Omega}\right]_{\mathrm{ELP}}=\frac{1}{v}\left[\frac{d\sigma}{d\Omega}\right]_e J_P(p_z)\,,$$
$$p_z v=\tfrac{1}{2}v^2-\tfrac{1}{2}k^2-|\epsilon_i|\,. \tag{3}$$

Here $(d\sigma/d\Omega)_e$ is the cross section for elastic scattering of an electron with velocity $\vec{v}$ at a target nucleus with charge Z_T. Though Eq. (3) has been derived imagining the ELP as the BEP in the projectile rest frame, it has been shown by Jakubassa[14] that Eq. (3) holds even if $Z_p<Z_T$. If at large velocities v the Born approximation is valid, screening of the ionizing target nucleus is easily incorporated by substituting in $(d\sigma/d\Omega)_e$ the charge Z_T by $Z_T-F(q)$, where $F(q)$ is the coherent atomic scattering factor[15] and $q=2v\sin(\theta/2)$ the elastic momentum transfer.

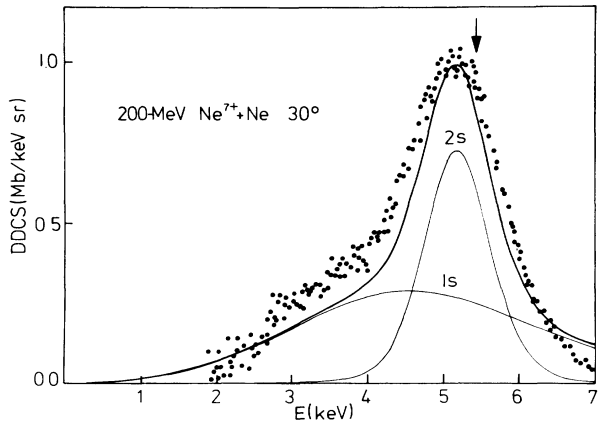

FIG. 10. Comparison of experimental ELP data (Ref. 16) with CP's from Hartree-Fock calculations of the neutral neon atom (Ref. 9). The energy position of the CP has been adjusted as described in the text. Individual shell contributions of the $(1s)^2(2s)^1$ Ne^{7+} state are shown.

Figure 10 shows experimental results from Prost *et al.*[16] for the ELP from 200-MeV Ne^{7+} on Ne at $\theta=30°$. The solid curves are obtained from Eq. (3) where the neutral Hartree-Fock CP's (Ref. 9) have been shifted by the ionization energies of the highly ionized Ne^{7+} ion.[17] In Fig. 10 the position of the neutral neon CP is indicated by an arrow which demonstrates the drastic energy shift due to the large excitation stage. In order to coincide experimental data points and theoretical curves an additional shift of about 50 eV had to be applied. This shift may indicate a Compton defect as discussed with reference to Fig. 8. Figure 10 clearly demonstrates that the large ionization degree not only shifts the CP's to lower electron energies but also that the CP's from Hartree-Fock calculations for neutral atoms[9] are too narrow. Since the CP is dominated by the contribution of the remaining $2s$ electron in Ne^{7+} we have recalculated the ELP with a hydrogeniclike CP for the $2s$ state where we have replaced the nuclear charge Z_p by $Z_p-\sigma$. Figure 11 shows resulting ELP's with the screening constants $\sigma=0$,

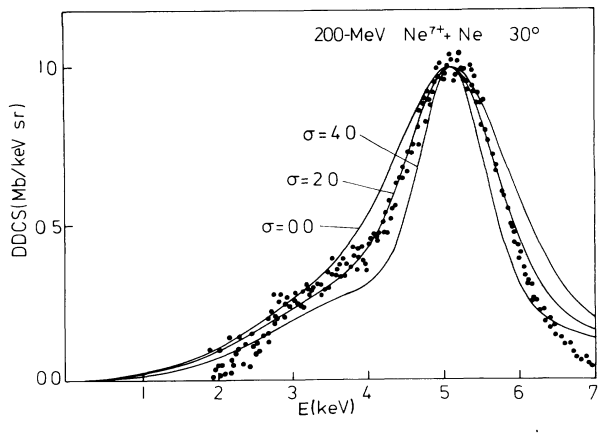

FIG. 11. CP's with hydrogenic $2s$ contribution for various inner-screening constants σ.

2, and 4. While $\sigma=4$ represents the Hartree-Fock calculation for the neutral atom very well, a fact which is well known from conventional γ-Compton scattering,[18] the pure hydrogenic case ($\sigma=0$) is too broad. In contrast, $\sigma=2$ reproduces the experimental data fairly well. In fact, $\sigma=2$ coincides with the naive picture that the two $1s$ electrons of Ne^{7+} completely screen two nuclear charges for a $2s$ electron.

IV. CONCLUSION

In conclusion the DDCS of the BEP is given by the Rutherford cross section of scattering an electron with initial momentum $\vec{p}$ into $d\Omega$ by a projectile with charge Z_p and velocity $\vec{v}$ times the probability that an electron with momentum $\vec{p}$ exists. The ELP is either understood as a BEP in the projectile rest frame or as the elastic scattering cross section for an electron with initial velocity $(\vec{v}+\vec{p})$ by a screened target nucleus Z_T into $d\Omega$ times the probability that such an electron exists.[19] In both cases it follows from energy and momentum conservation that the probabilities are represented by CP's.

In this 50th anniversary year of Bethe's famous review article in Handbuch der Physik on one- and two-electron atoms, it might be appropriate to remember that the CP's are nothing more than the Bethe-ridge of the generalized oscillator strength.[20,21]

[1]F. Bell, H. Böckl, M. Z. Wu, and H. D. Betz, J. Phys. B 16, 187 (1983).
[2]C. Dal Cappello, C. Tavard, and A. Lahmam-Bennani, Phys. Rev. A 26, 2249 (1982).
[3]*Compton Scattering,* edited by B. Williams (McGraw-Hill, New York, 1977).
[4]A. D. Barlas, W. H. E. Rueckner, and H. F. Wellenstein, J. Phys. B 11, 3381 (1978).
[5]M. E. Rudd, C. A. Sautter, and C. L. Bailey, Phys. Rev. 151, 20 (1966).
[6]L. H. Toburen and W. E. Wilson, Phys. Rev. A 5, 247 (1972).
[7]M. E. Rudd and J. H. Macek, *Case Studies in Atomic Physics* (North-Holland, New York, 1974), Vol. III, p. 49.
[8]M. E. Rudd, L. H. Toburen, and N. Stolterfoht, At. Data Nucl. Data Tables 18, 413 (1976); 23, 405 (1979).
[9]F. Biggs, L. B. Mendelsohn, and J. B. Mann, At. Data Nucl. Data Tables 16, 201 (1975).
[10]P. Eisenberger and P. M. Platzman, Phys. Rev. A 2, 415 (1970).
[11]T. C. Wong, L. B. Mendelsohn, H. Grossman, and H. F. Wellenstein, Phys. Rev. A 26, 181 (1982).
[12]C. E. Kuyatt and T. Jorgensen, Phys. Rev. 130, 1444 (1963).
[13]J. E. Miraglia and V. H. Ponce, J. Phys. B 13, 1195 (1980).
[14]D. H. Jakubassa, J. Phys. B 13, 2099 (1980).
[15]D. T. Cromer and J. T. Waber, *International Tables for X-Ray Crystallography* (Kynoch, Birmingham, England, 1974), Vol. IV, Table 2.2A, p. 71.
[16]M. Prost, D. Schneider, R. DuBois, P. Ziem, H. C. Werner, and N. Stolterfoht, *Nuclear Methods Monographs 2,* edited by Berényi and G. Hock (Elsevier, Amsterdam, 1982), p. 99.
[17]T. A. Carlson, C. W. Nestor, N. Wassermann, and J. D. McDowell, At. Data 2, 63 (1970).
[18]L. Mendelsohn and V. H. Smith in *Compton Scattering,* edited by B. Williams (McGraw-Hill, New York, 1977), p. 109.
[19]D. Burch, H. Wieman, and W. B. Ingalls, Phys. Rev. Lett. 30, 823 (1973).
[20]H. Bethe, *Handbuch der Physik,* edited by H. Geiger and K. Scheel (Springer, Berlin, 1933), Vol. 24/1, p. 273.
[21]M. Inokuti, Rev. Mod. Phys. 43, 297 (1971).